Japan Geoscience Union Meeting 2014
(28 April - 02 May 2014 at Pacifico YOKOHAMA, Kanagawa, Japan)

SSS31-01 Room:502 Time:April 30 14:15-14:30

Basement structure beneath the Tokyo metropolitan area as revealed with the MDRS method

HORIKAWA, Haruo[1*] ; ABE, Shintaro[1] ; YAMAGUCHI, Kazuo[1] ; NODA, Katsuya[2] ; ABE, Susumu[2]

[1]AIST/GSJ, [2]JGI

We applied the multi-dip reflection surfaces (MDRS) method to seismic data originally acquired by the Tokyo Metropolitan Government, and successfully revealed the shape of basin floor and geological structure above the basin floor. The resultant seismic image is interpreted as rift geometry with imbricated normal faults. Moreover, the active Tachikawa fault seemingly has a high dip angle.

The Kanto region that includes the Tokyo Metropolitan area is located near the boundary between the northeastern Japan and the southwestern Japan, and has complicated tectonic history. Moreover, the region is covered with thick sediment of Neogene to Quaternary. Seismic profiling has contributed to revealing the structure such as concealed half-graben and tectonic history.

The MDRS method is an improvement on the common reflection surface stacking (CRS) method in that the MDRS method can deal with conflicting dipping events. The CRS method can detect subtle reflection events by stacking the data along a specific reflection surface. However, complex geological structure often yields a seismic wave field that contain events from various surfaces with different geometry, and the CRS method has difficulty in resolving such complicated reflection events. The MDRS method seeks subtle reflected events, repeatedly applying the CRS method with various sets of parameters that govern the character of reflection surfaces, and superimposes the derived seismic images with high values of semblance. Consequently, the MDRS method can provide a clear image of such complex geological structure.

Seismic data reprocessed in this study was acquired in the Tokyo metropolitan area. The seismic survey was conducted in order to clarify the depth of the top of pre-Neogene basement and the sedimentary structure above the basement. data processing with the conventional common mid-point stacking was performed in the original survey, and provided an image with vertical offset of the top of the basement that corresponds to the active Tachikawa fault, but it generated a poor image for the overall shape of the basin floor; we can only recognize that the basin floor is not flat.

On the contrary, the MDRS method successfully generated a clear image of the basin floor and the stratification of sediments just above the basin floor. The sediments are in a wedge shape, and contain reflectors with a fanning and upward shallowing of dips. The wedge-shaped sediments are aligned horizontally. We interpret this structure as rift system with imbricated normal faults. In fact, rift system has been recognized beneath the Kanto region that is believed to be formed during the Miocene associated with opening of the Sea of Japan. Moreover, we have newly found that the top of the basement extends further beneath the Tachikawa fault. This suggests that the Tachikawa fault has high dip angle.

Acknowledgement
The Civil Engineering Center of the Tokyo Metropolitan Government provided the seismic data reprocessed in this study.

Keywords: multi-dip reflection surfaces method, basement structure, seismic reflection survey, common reflection surface stacking

Japan Geoscience Union Meeting 2014
(28 April - 02 May 2014 at Pacifico YOKOHAMA, Kanagawa, Japan)

SSS31-02 Room:502 Time:April 30 14:30-14:45

Seismic velocity structure in Ou backbone range by using a dense seismic array

AOYAGI, Yasuhira[1*] ; KIMURA, Haruo[1]

[1]Central Research Institute of Electric Power Industry

Ou backbone range is a strain concentration zone with E-W contraction along NE Japan arc, hence forms one of the most active reverse-faulting zone in Japan. Some destructive earthquakes, such as the 1896 Rikuu earthquake (M7.2) and the 2008 Iwate-Miyagi nariku earthquake (M7.2), have occurred there for this century. Fault rupture of the 1896 Rikuu earthquake which occurred along the eastern margin of the Yokote Basin fault zone did not reach all over the fault zone but limited to its northern part. The purpose of this study is to find some crustal structures which could control a termination of fault rupture. In this presentation, we will discuss a property of seismic velocity structure which might terminate the fault rupture of some historical earthquakes based on seismic tomography using a dense arrayed micro-earthquake observation data.

Keywords: Ou backbone range, Seismic velocity structure, Rupture termination, Micro-earthquake observation, Seismic tomography

Japan Geoscience Union Meeting 2014
(28 April - 02 May 2014 at Pacifico YOKOHAMA, Kanagawa, Japan)

SSS31-03 Room:502 Time:April 30 14:45-15:00

Relation between the resistivity structure around Hakone volcano and seismicity induced by the 2011 Tohoku Earthquake

YOSHIMURA, Ryokei[1*] ; OGAWA, Yasuo[2] ; YUKUTAKE, Yohei[3] ; KANDA, Wataru[2] ; KOMORI, Shogo[4] ; GOTO, Tadanori[5] ; HONDA, Ryou[3] ; HARADA, Masatake[3] ; YAMAZAKI, Tomoya[1] ; KAMO, Masato[1] ; YASUDA, Yojiro[6] ; TANI, Masanori[5]

[1]DPRI, Kyoto University, [2]Volcanic Fluid Research Center, Tokyo Institute of Technology, [3]Hot Springs Research Institute of Kanagawa Prefecture, [4]Institute of Earth Sciences, Academia Sinica, [5]Graduate School of Engineering, Kyoto University, [6]Graduate School of Engineering, Tottori University

Seismicity around the Hakone volcano was activated just after the arrival of surface waves caused by the 2011 off the Pacific coast of Tohoku Earthquake. Most of these triggered earthquakes had similar distribution to prior occasional swarm activities. In order to image electrical properties around such seismic events, we carried out audio-frequency magnetotelluric (AMT) measurements at 39 sites in December 2011 (Yoshimura et al., 2012). In this study, we conducted 3D modeling of dense AMT (Yoshimura et al., 2012) and MT (Ogawa et al., 2012) data, to figure out electrical characteristics around the triggered seismicity. In spite of careful treatments for noise reduction, the effects of noise were still seen on the longer parts of the responses ($<$1 Hz) at the several measurement sites. Thus we determined to have use of the frequency range from 320 Hz to 1.02 Hz. The full components the impedance tensors at 51 sites in total were inverted using the code developed by Siripunvaraporn et al. [2005]. The model space consists of 64(x-)$\times$46(y-)$\times$36(z-direction; including 7 air layers) blocks. The minimum horizontal size of blocks was 400m$\times$400m. Significant characteristics of the obtained three-dimensional resistivity model are: (1) the most of the triggered earthquakes, which occurred shallower than a depth of 4km, seem to align along edges or areas just inside the relatively resistive block; (2) surface conductive blocks, in which there were very few earthquakes, were observed beneath not only fumarolic areas but geothermal non-active regions.

Keywords: magnetotellurics, three-dimensional resistivity structure, Hakone volcano, triggered earthquake

Japan Geoscience Union Meeting 2014
(28 April - 02 May 2014 at Pacifico YOKOHAMA, Kanagawa, Japan)

SSS31-04 Room:502 Time:April 30 15:00-15:15

Three-dimensional seismic velocity structure around the Neodani fault

NAKAJIMA, Junichi[1*] ; KATO, Aitaro[2] ; IWASAKI, Takaya[2] ; THE JAPANESE UNIVERSITY GROUP OF THE, Joint seismic observations at the are[3]

[1]Graduate School of Sci., Tohoku Univ., [2]ERI, Univ. of Tokyo, [3]The Japanese University Group of the Joint Seismic Observations at the Area of Nobi Earthquake

The joint research project started in 2007 to enhance our knowledge on the deep structure around the Neodani fault, along which the largest crustal earthquake, the Nobi earthquake (M8.0), occurred in 1891. As a part of the project, 73 seismograph stations were installed around the fault, resulting in a dense seismograph network with a spatial separation of ˜10 km.

We performed a travel-time tomography to reveal a detailed 3D velocity structure around the Neodani fault. The tomographic method of Zhao et al. (1992) was applied to arrival-time data of earthquakes (N=3027) that occurred from 2002 to January 2013. The total number of arrival-time data was 248,354 for P waves and 215,034 for S waves. Horizontal grid nodes spaced at intervals of 0.1 degrees were set in the study area and vertical grid nodes were set at intervals of 5?30.

The obtained results show interesting features in terms of heteroegensou structures beneath the source area of the Nobi earthquake.

1. The lower crust beneath the Nobi plain shows low Vp and Vs compared to surrounding areas.
2. A low Vp and Vs area is imaged continuously from the Philippine Sea slab and the mid crust beneath the Nobi earthquake.
3. The lower crust beneath the Neodani fault shows an along-fault variation in seismic velocities, with moderate- to high-velocity crust to the southeast and low-velocity crust to the northwest.

Japan Geoscience Union Meeting 2014
(28 April - 02 May 2014 at Pacifico YOKOHAMA, Kanagawa, Japan)

SSS31-05 Room:502 Time:April 30 15:15-15:30

Stress tensor inversion in the Nobi fault area, Central Honshu, Japan

KATSUMATA, Kei[1*] ; KOSUGA, Masahiro[2] ; KATAO, Hiroshi[3] ; YAMADA, Takuji[1] ; KATO, Aitaro[4] ; THE JAPANESE UNIVERSITY GROUP, The joint seismic observations[4]

[1]Inst. Seismo & Volcano, Hokkaido Univ., [2]Earthquake and Volcano Observatory, Graduate School of Science and Technology, Hirosaki University, [3]Research Center for Earthquake Prediction, Disaster Prevention Research Institute, Kyoto University, [4]Earthquake Research Institute, University of Tokyo

A stress tensor inversion method was applied to 702 focal mechanism solutions in the Nobi fault area, Central Honshu, Japan, which are obtained by using HASH (Hardebeck and Shearer, 2002) that is a method using a first motion polarity of P-wave as data. The study area, 35.3-36.1N and 136.0-137.0E, is gridded with 0.1 X 0.1 spacing in the east-west and north-south directions, respectively. The focal mechanisms are divided into three groups according to the depth of hypocenter: 2-7 km, 5-10km, and 8-13km. From each group the focal mechanisms are selected that the epicenters are located within a radius of 15 km centered at each grid. The SATSI is applied to the data at each group of depth, which is a stress tensor inversion method developed by Hardebeck and Michael (2006). The spatial pattern of stress is obtained at each depth: 2-7 km, 5-10km, and 8-13km. We find that (1) the maximum principal stress (σ_1) is oriented east-west direction almost all over the study area, and (2) the σ_1 direction rotates clockwise by some tens degrees around the Nobi fault.

Keywords: Nobi fault, joint seismic observations, focal mechanism, stress tensor inversion, inland earthquake, active fault

Japan Geoscience Union Meeting 2014
(28 April - 02 May 2014 at Pacifico YOKOHAMA, Kanagawa, Japan)

SSS31-06 Room:502 Time:April 30 15:30-15:45

Strain concentration zone recognized from GNSS data in the San-in region

NISHIMURA, Takuya[1*]

[1]Disaster Prevention Research Institute, Kyoto University

Introduction

In the San-in region, southwest Japan, there were many large earthquakes including the 1943 M7.2 Tottori and the 2000 M7.3 Western Tottori prefecture earthquakes in the shallow crust. It is well-known that an active zone of microseismicity exists parallel to the coastline of Sea of Japan. On the other hand, recent geodetic data acquired by the GEONET (GNSS Earth Observation Network) suggest that a rate of contemporary deformation is small in the Chugoku district including the San-in region (e.g., Sagiya *et al.*, 2000). We study a detailed pattern of crustal deformation using the GEONET data to clarify a relation between contemporary deformation and microseismicity.

Method

We used daily coordinates of the GEONET GNSS stations published by the Geospatial Information Authority of Japan (F3 solution). We fit a function of linear, annual, and semi-annual components to time-series of site coordinates relative to site 950462 (Fukue) to estimate secular site velocities. We also estimate strain distribution at grid points (Shen *et al.*, 1996) and in Delaunay triangles using the site velocities.

Result

We identify a concentration zone of deformation corresponding to the active zone of microseismicity in an eastern part of the San-in region during April 2005 and December 2009. Distribution of maximum shear strain rate shows that an eastern inland part of the Chugoku district has the lowest strain rate (10^{-8} yr^{-1}) in the Japanese Islands and that the high strain rate (10^{-7} yr^{-1}) is distributed in a band along the coast of Sea of Japan. High strain rate is also observed in a vicinity of the source area of the 2000 Western Tottori prefecture earthquake, which suggests postseismic deformation of the 2000 earthquake is still continuing.

Velocity profile across the active zone of microseismicity shows a velocity component parallel to the active zone (N80^{o}E) has an offset of 2 mm/yr in and around the active zone. Movements across the offset suggest a right-lateral strike slip, which is consistent with a typical focal mechanism of shallow crustal earthquakes in the zone. The 2011 Tohoku-oki earthquake affects crustal deformation in the San-in region. In a postseismic period from January 2012 to December 2013, the strain rate in the San-in region became twice as large as that before 2011.

The deformation can be roughly explained by a right-lateral block motion across the active zone of microseismicity. The used GNSS network is too sparse to estimate a locking depth of a fault between the blocks. A dense GPS array is necessary for more detailed analysis.

Concluding remarks

Analysis of the GEONET data identifies a strain concentration zone corresponding to the active zone of microseismicity along the coast of Sea of Japan in an eastern part of the San-in region. This zone with a width of ˜10 km accommodates right-lateral strike-slip movement of 2 mm/yr, which is concordant with a focal mechanism of shallow earthquakes. The observed strain rate doubled after the 2011 Tohoku-oki earthquake. More detailed distribution of deformation in the strain concentration zone is important to clarify the deformation mechanism. We need to study with both observation and model calculation.

Reference

Sagiya *et al*., PAGEOPH, 147, 2303-2322, 2000
Shen *et al.*, JGR, 101(B12), 27957-27980, 1996

Keywords: Crustal deformation, Strain concentration zone, GNSS, the San-in region

Japan Geoscience Union Meeting 2014
(28 April - 02 May 2014 at Pacifico YOKOHAMA, Kanagawa, Japan)

SSS31-07 Room:502 Time:April 30 16:15-16:30

HV frictional strength of wet Longmenshan fault gouge and its comparison with the temperature anomaly in WFSD drill hole

TOGO, Tetsuhiro[1*] ; SHIMAMOTO, Toshihiko[1] ; MA, Shengli[1] ; YAO, Lu[1]

[1]Institute of Geology, China Earthquake Adiministration

Estimation of frictional strength from temperature anomaly along coseismic fault in a drill hole after a large earthquake has received much attention recently (e.g., J-FAST project in Japan Trench after the Tohoku-oki earthquake. Surface ruptures more than 250 km long formed along existing Yingxiu-Beichuan fault, a major fault in the Longmenshan fault system, during the 2008 Wenchuan earthquake (Mw = 7.9). Drilling was conducted at Hongkou in Dujiangyan city, a western part of the fault, as a part of Wenchuan Earthquake Fault Scientific Drilling (WFSD). Temperature monitoring is an important task in the project, and WFSD-1 hole was drilled within one year after the earthquake (fastest drilled hole after a large earthquake in the world). Drilling revealed a large scale fault zone for the depth range of 580˜760 m, consisting of cataclasites (about 10 m wide), many thin fault gouge zones and fault breccia (Li et al., 2013, Tectonophysics). Temperature anomaly of only 0.15 degrees Centigrade was recognized at a depth of 590 m along a presumed coseismic slip zone (evidence for coseismic slip zone is not so strong though). Mori et al. (2010, AGU) report friction coefficient less than 0.03 from this temperature anomaly. This friction coefficient was even lower than low friction coefficients (typically 0.05˜0.2) at high slip rates, reported in the last two decades.

We have conducted wet gouge experiments on foliated fault gouge containing 25 wt% of water with Teflon sleeve at slip rates to 1.3 m/s and at normal stresses of 1.0˜4.8 MPa, and compared the results with those on dry gouge with room humidity. Sample was collected from the Hongkou outcrop (see Togo et al., 2011a, EQS), only several hundred meters from the WFSD-1 drill site. Wet gouge has peak friction coefficient of 0.1˜0.36 and steady-state friction coefficient of 0.03˜0.14, as compared with 0.65˜0.8 and 0.15˜0.2 for dry gouge (Togo et al., 2011b, EQS). Wet gouge is substantially weaker than dry gouge, but its frictional strength is still somewhat greater than expected from the near absence of temperature anomaly. However, normal stress expected at the depth of temperature anomaly is expected to be more than twice as high as those of our experiments (experiments could not be done at higher normal stresses due to gouge leak). Both peak and steady state friction coefficients of wet gouge tend to decrease by a power low with increasing normal stresses and the extrapolated steady state friction coefficient at the drilling depth reached from 0.028 to 0.022, which results are consistent with the result by Mori et al. (2010). Thus wet gouge has frictional strength fairly close to that expected from the temperature anomaly.

Wet and dry gouges have completely different deformation textures. Deformed dry gouge is characterized by ultrafine-grained slip zones (typically several to a few tens of microns thick) and weakly deformed gouge. Overlapped slip-zone structures are very common in sheared dry gouge. On the other hand, slight grain-size refinement occurs in wet gouge, and the whole wet gouge zone remains only weakly deformed. We consider that the build-up of pore pressure due to compaction induced and/or thermal pressurization separated grains and suppressed grain crushing in wet gouge.

Keywords: High-velocity friction experiment, Longmenshan fault, Wenchuan earthquake, Frictional heating, Bore hole temperature measurement

Japan Geoscience Union Meeting 2014
(28 April - 02 May 2014 at Pacifico YOKOHAMA, Kanagawa, Japan)

SSS31-08 Room:502 Time:April 30 16:30-16:45

Numerical simulation of shear bands formation in ground due to strike-slip fault

NODA, Toshihiro[1*] ; YAMADA, Shotaro[1] ; ASAOKA, Akira[2] ; SAWADA, Yoshihiro[2] ; KAWAI, Yuta[1]

[1]Nagoya University, [2]Association for the Development of Earthquake Prediction

When a strike-slip fault occurs, flower structures denoting petaloid patterns of shear bands appear inside the ground above the fault, and also the Riedel shear structures showing en-echelon shear bands appear on the surface of the ground. Ueda[1)] conducted model experiments accounting a strike-slip fault and showed evolution process of shear bands inside the model ground using X-ray CT scan system. Also, Sawada and Ueda[2)] numerically simulated evolution of flower structures etc., using a large-deformation analysis where an elasto-perfectly plastic model with the Mohr Coulomb failure criteria was used.

In this study, referring the research work by Sawada and Ueda[2)], evolution of shear bands was numerically investigated by using a soil-water coupled finite deformation analysis code ***GEOASIA***[3)] on which the SYS Cam-clay[4)] was mounted as an elasto-plastic soil model. In the analysis, since the rate-type equation of motion is precisely time-integrated, progressive failure will be analyzed as a nonlinear dynamic problem, and then generation and/or propagation of waves induced by shear bands formation[5)] will also naturally be developed in the analysis. The constitutive model used is capable of describing a wide variety of soils within the same theoretical framework. Here are shown numerical examples in which soil is taken as a non-coupled material with liquid.

First considered was a 3D FE mesh with one element in strike direction of a fault (i.e. y-direction) shown in Fig.1. The right-lateral strike-slip fault was assumed to be located below the three elements at the mid bottom of the ground. As for the boundary conditions, periodic boundary was taken directly above the fault on the x-z planes of the ground, and displacement was applied to the y-direction on the other parts of the x-z planes with a constant rate of 10^{-6}m/s on the opposite side across the fault. Also, x-z and y-z planes were frictionless. In this case, the ground exhibited localization of deformation and the shear bands grow from the bottom in a logarithmic spiral manner (“ flower structures ”). Then, the formation was attributed to plastic swelling behavior of soil element.

Next used were the other 3D meshes with forty elements in the strike direction (Fig.2) so as to investigate evolution of shear bands and effect of homogeneity/initial-imperfection in ground on the evolution. Here, as the boundary conditions, periodic boundary was assumed on the mutually opposite x-z planes and displacement was applied to the nodes located at the bottom with the same rate on the opposite side across the fault, while the same material constants were used. The imperfection was given to some elements directly above the fault by slightly altering a material constant of them. In the imperfection case, flower structures occurred inside the ground, thereafter Riedel shear structures appeared on the surface. The parts of the Riedel shear exhibited more significant upheavals than its surroundings. Furthermore, in the other numerical cases, angle between the Riedel shear and the strike varied with the different material constant.

1) Ueda K.(2003): Evolution of strike-slip fault systems and associated geomorphic structures: Model Test, CRIEPI Rep. No.U03021, in Japanese.

2) Sawada, M. & Ueda K.(2009): Numerical simulation for evaluation of structure zone distribution due to strike-slip fault, CRIEPI Rep.No.N08028, in Japanese.

3) Noda, T. et al.(2008): Soil-water coupled finite deformation analysis based on a rate-type equation of motion incorporating the SYS Cam-clay model, Soils and Foundations, 48(6), 771-790.

4) Asaoka, A.et al.(2002): An elasto-plastic description of two distinct volume change mechanisms of soils, Soils and Foundations, 42(5), 47-57.

5) Noda, T. et al.(2013): Acceleration generation due to strain localization of saturated clay specimen based on dynamic soil-water coupled finite deformation analysis, Soils and Foundations, 53(5), 653-670.

Keywords: strike-slip fault, shear bands, Riedel shear, flower structure, numerical analysis

SSS31-08 Room:502 Time:April 30 16:30-16:45

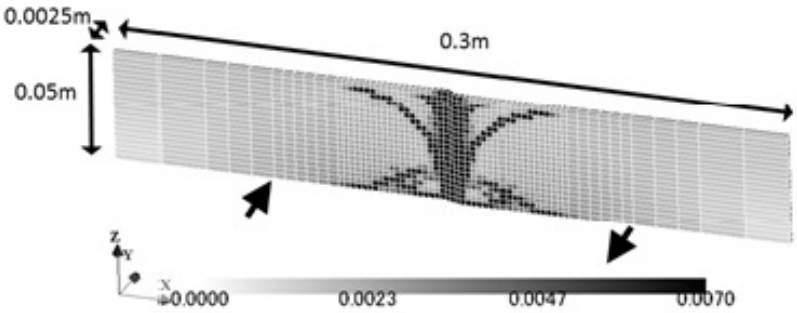

Fig.1. Occurrence of flower structure

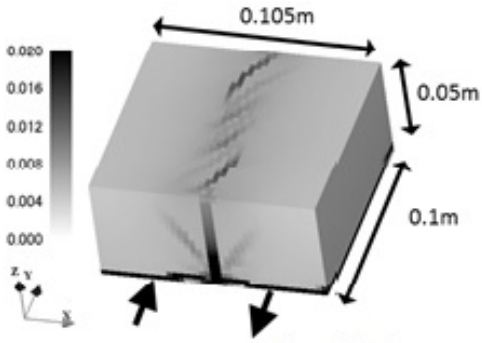

Fig.2. Occurrence of Riedel shear after flower structure, ground with initial material imperfection

Japan Geoscience Union Meeting 2014
(28 April - 02 May 2014 at Pacifico YOKOHAMA, Kanagawa, Japan)

SSS31-09 Room:502 Time:April 30 16:45-17:00

Spatially inhomogeneous stress field in the source area of the 2011 Fukushima Hamadori earthquake sequence

YOSHIDA, Keisuke[1*] ; HASEGAWA, Akira[1] ; OKADA, Tomomi[1]

[1]Research Center for Prediction of Earthquakes and Volcanic Eruptions, Tohoku University

After the 2011 great Tohoku-Oki earthquake, many earthquakes occurred near Iwaki, Fukushima Prefecture, including Mw6.8 event of April 11. This 2011 Fukushima Hamadori earthquake sequence is characterized by normal faulting, with T-axis oriented in the NW-SE, E-W and NE-SW directions for events in the northern, central and southern parts of the source area, respectively.

In order to understand the cause of such a remarkable spatial variation of focal mechanisms, we investigated the stress field in the source area of this earthquake sequence. First, we relocated hypocenters of events that occurred during the period from 1997 to 2012 by the double-difference location method. Relocated hypocenters show that events near the 3/19 Mw 5.8 earthquake in the southern area, those near the 3/23 Mw 5.7 earthquake in northern area and those near the 4/11 Mw 5.9 earthquake in central area are aligned along planes dipping westwards corresponding to one of nodal planes, respectively.

Then, we estimated the stress field in the source area of the sequence by a stress tensor inversion of focal mechanisms reported by the National Research Institute for Earth Science and Disaster Prevention and Japan Meteorological Agency. Results show that the stress field is very heterogeneous in space with normal fault stress regime after the occurrences of the main-shock of each part of the source area. In the northern, central, southern and east parts of the source area, the minimum principal stress ($\sigma 3$) axes are oriented in the NW-SE, E-W, NE-SW and NNE-SSW directions, respectively. As a whole, $\sigma 3$ axis shows the concentric circle-like distribution. In contrast, before the occurrence of the main-shock of each part, $\sigma 3$ axis is oriented homogeneously in space in the E-W direction.

This observation suggests the possibility that the remarkable heterogeneity in stress field is caused by the static stress change of large earthquakes. We estimated the static stress changes caused by the 2011 Fukushima Hamadori earthquake sequence. A slip model estimated by Hikima (2012) using strong motion waveforms was used for the Mw6.8 earthquake. Furthermore, we made fault models of the 3/19 Mw 5.7, 3/23 Mw 5.8 and 4/12 Mw 5.7 events using hypocenter locations and the scaling relation between moment magnitude, fault length, width and slip amount for estimating their static stress changes.

Spatial distribution of $\sigma 3$ axis direction of the static stress change is approximately the same as that of the observed stress field after the occurrences of the main-shock of each part of the source area. This strongly suggests that $\sigma 3$ axis rotated after the 2011 Fukushima Hamadori sequence and the stress magnitude in the focal area before the sequence was smaller than the static stress change ($<$˜several MPa). We estimated the differential stress magnitude assuming that the difference in the stress tensor before and after the earthquakes is equal to the static stress change associated with the large earthquakes. Estimated magnitude of the differential stress was $<$20 MPa.

Keywords: crustal stress, focal mechanism, weak fault

Japan Geoscience Union Meeting 2014
(28 April - 02 May 2014 at Pacifico YOKOHAMA, Kanagawa, Japan)

SSS31-10 Room:502 Time:April 30 17:00-17:15

To what degree can rocks become weak during deformation?: Fracturing-dissolution-mass transfer-precipitation creep

TAKESHITA, Toru[1*] ; OKAMOTO, Ayumi[1]

[1]Hokkaido University

The megaquake underneath the pacific ocean off the northeast Japan revealed important facts on crustal dynamics of the Japanese island. Among them, a new suggestion on the magnitude of differential stress in the crust is important. After the megaquake, peculiar earthquakes occurred in places, where earthquakes do not frequently occur. A typical example was an earthquake caused by normal faulting near the Iwaki-city, northeast Japan, where the stress field of a weak E-W compression was changed to that of an E-W extension. Based on the facts, Yoshida et al. (2012) estimated that the magnitude of differential stress was on the order of 1 MPa in upper crust. In this presentation, we will discuss the newly arising problems of crustal dynamics in Japanese islands, and also whether or not rocks can be deformed by such low differential stresses (i.e. *c.* 1 MPa), if this estimate of flow stresses is in fact correct.

We have been studying deformation processes and mechanisms in rocks at brittle ductile transition conditions, which seem to control the strength of upper crust, based on microstructural analyses in naturally deformed rocks. Deformation behaviors at the conditions of brittle-ductile conditions can be observed in metamorphic rocks formed at great depths, because these are elevated from ductile to brittle regions across the depth of brittle-ductile transition. For example, pervasive semi-brittle micro-faulting occurred in quartz schist from the Sambagawa metamorphic rocks at brittle ductile transition conditions. Here, although quartz layers were truncated by micro-faults, very-fine grained dynamically recrystallized quartz grains were also formed along them (i.e. micro-shear zone), suggesting components of ductile deformation. Further, very-fine-grained white mica was formed along the micro-faults, suggesting fluid percolation. With increasing deformation, the density of micro-faults increased, accompanied by the widening of micro-shear zones and associated decrease of the volume fraction of undeformed lenses. Perhaps, dissolution-precipitation creep dominated in micro-shear zones, having led to stress concentration in undeformed lenses, which were subsequently fractured. It is inferred that the rocks became softened with the increasing volume fraction of micro-shear zones.

Similarly, broken and displaced quartz detrital grains are observed in meta-sandstones deformed at brittle-ductile conditions from the Kamuikotan metamorphic rocks, northern Japan. Fibrous overgrowth of quartz occurred between the broken and displaced fragments of quartz, which appears as if these grains themselves restore the original shape. On the other hand, embayment occurred toward quartz grain sides at the boundary between quartz and white mica grains, suggesting dominant dissolution of quartz at this type of boundaries. Further, cataclasites formed along the Median Tectonic Line at the conditions of brittle-ductile conditions in the Cretaceous, and new minerals precipitated from fluids in the space created by fracturing and displacement of protolith forming minerals. The fracturing is accompanied by element migration via fluids, thus the degree increases with increasing degree of fracturing. In conclusion, deformation occurred by dissolution-mass transfer-precipitation assisted by fracturing under the conditions of brittle-ductile transition, by which significant weakening can be generated in rocks.

Keywords: differential stress in the upper part of crust, strain softening, micro-fracturing, dissolution, mass transfer, precipitation of minerals

Japan Geoscience Union Meeting 2014
(28 April - 02 May 2014 at Pacifico YOKOHAMA, Kanagawa, Japan)

SSS31-11 Room:502 Time:April 30 17:15-17:30

Detecting the stress condition at a fault from focal mechanism: application to the 2013 Awaji Island earthquake (M6.3)

MATSUMOTO, Satoshi[1*] ; KATAO, Hiroshi[2] ; IIO, Yoshihisa[2]

[1]Institute of Seismology and Volcanology, Kyushu Univ., [2]Disaster Prevention Research Institute, Kyoto Univ.

One of the approaches used to evaluate potential of an earthquake occurrence is the detection of stress concentration at an earthquake fault. Stress fields in stages for pre- and post-seismic event will be different from one another. However, this change cannot provide information regarding the potential for an earthquake to occur. Here, we propose a detection method for stress conditions that uses focal mechanism data. The condition can be defined both by background stress and by a moment tensor equivalent to the stress concentration. We apply this method to actual focal mechanism data from the Awaji Island earthquake (M6.3), Japan, and show the presence of stress concentration around the earthquake fault before the mainshock. In addition, the regional shear stress is shown to be ∼25 MPa in the area, implying that the stress level is still high, thus the potential for further seismicity in the area could be high.

Keywords: stress field, earthquake fault, focal mechanism

Japan Geoscience Union Meeting 2014
(28 April - 02 May 2014 at Pacifico YOKOHAMA, Kanagawa, Japan)

SSS31-12 Room:502 Time:April 30 17:30-17:45

A friction to flow constitutive law and its application to a two-dimensional modeling of earthquake cycles

SHIMAMOTO, Toshihiko[1*] ; NODA, Hiroyuki[2]

[1]Institute of Geology, China Earthquake Administration, [2]JAMSTEC

Establishment of a constitutive law from friction to high-temperature plastic flow has long been a task for solving problems such as modeling earthquakes and plate interactions. A linear combination of friction and flow laws disagrees with experimental data. Here we propose an empirical constitutive law that describes this transitional behavior with good agreements with experimental data on halite shear zones. A complete spectrum of properties including steady-state and transient behaviors can be predicted if friction and flow parameters are known. We show numerical models of seismic cycles of a fault across the lithosphere as an application. Our friction-to-flow law merges brittle-plastic Christmas-tree strength profiles of the lithosphere and rate-dependency fault models used for earthquake modeling on a unified basis. Conventionally strength profiles were drawn assuming a strain rate for the flow regime, but we emphasize that stress distribution evolves reflecting the fault behavior. Previous fault models are revised based on our earthquake modeling. Seismic fault motion is followed by fault creep in the transitional regime and this explains pseudotachylytes overprinted by mylonitic deformation, reported at various places in the world.

Keywords: Friction to flow constitutive law, Earthquake cycle modeling, Fault model, Lithosphere rheology, Mylonite, Pseudotachylite

Japan Geoscience Union Meeting 2014
(28 April - 02 May 2014 at Pacifico YOKOHAMA, Kanagawa, Japan)

SSS31-13 Room:502 Time:April 30 17:45-18:00

A consideration about computation of tectonic stress field for inland thrust earthquake

MIYATAKE, Takashi[1]*

[1]ERI, The Univ. of Tokyo

In the case of pure thrust earthquake, the driving stress system is expected to have been as shown in Fig.1a. The stress in this figure is tectonic stress; thus, the lithostatic pressure σ_V(=ρgh) must be added. The tectonic system (Fig. 1a) can be decomposed into two systems (Fig. 1b): A and B. The functional forms of σ_X and σ_Y are unknown. The assumption that that σ_X is uniform in system A causes almost uniform shear and normal stresses on the fault. Strength (peak stress) and dynamic friction can be estimated when σ_V (=ρgz) is added to the fault normal stress and the resultant normal stress is multiplied by static and dynamic frictional coefficients. Under these conditions, we found a large stress drop in the shallower parts and minimum strength excess at the free surface. This suggests that the earthquake rupture must have started at the surface and that the stress drop must have been the highest at the ground surface. These results can be avoided if the stress σ_X is assumed to increase with depth. The depth dependency is related to variations in elastic constants. The stress field in this region likely originated primarily from plate motions. Therefore, we selected the displacement boundary condition $u_X=u_0$, which correspondings to system A' in Fig. 1c. It should be noted that other displacement components were not fixed, but free stress conditions (except the σ_{xx} component) were imposed according. After solving the stress field imposing the above boundary condition, the resultant stress component σ_{xx} was added on the boundary of $x=\pm L_X$ as a further boundary condition. The solution is the same as the problem in which the boundary condition is imposed. Taking the linear elasticity into account, the target solution can be estimated by superposing solutions A and B in Fig. 1b. System A is equivalent to system A'. The effect of system B on fault normal and shear stress is expected to be negligible, because these stresses are exactly zero for a uniform structure. We estimated such effects in a heterogeneous structure by assuming that the value of σ_Y=σ_{yy} (z) on the boundary of $y=\pm L_y$ is the same as σ_{xx} (z) on the boundary of $x=\pm\pm L_x$. We found system B to exert little effect (less than 5%) on the stress components of σ_{zx}, σ_{xx}, and σ_{zz}. Thus, B had little effect on fault normal and shear stress on the fault plane, where σ_{xx} (z) is the averaged stress component along the y-axis on the corresponding boundaries. Based on the condition of thrust earthquake that $||\sigma_X|>|\sigma_Y|>|\sigma_Z|$(Fig. 1a), the above mentioned σ_{zx}, σ_{xx}, and σ_{zz} were overestimated in our study. Thus, we can ignore the effects of system B.

Keywords: inland earthquake, stress field